Differentiation 83 (2012) 249–259

Contents lists available at SciVerse ScienceDirect

Differentiation

journal homepage: www.elsevier.com/locate/diff

In vitro and *in vivo* osteogenesis of human mesenchymal stem cells derived from skin, bone marrow and dental follicle tissues

Bong-Wook Park [a], Eun-Ju Kang [b], June-Ho Byun [a], Myeong-Gyun Son [a], Hyun-Joon Kim [c], Young-Sool Hah [d], Tae-Ho Kim [b], B. Mohana Kumar [b,e], Sun-A Ock [b,f], Gyu-Jin Rho [b,e,*]

[a] *Department of Oral & Maxillofacial Surgery, School of Medicine and Institute of Health Science, Gyeongsang National University, Jinju 660-701, Republic of Korea*
[b] *OBS/Theriogenology and Biotechnology, College of Veterinary Medicine, Gyeongsang National University, Jinju 660-701, Republic of Korea*
[c] *Department of Anatomy, School of Medicine, Gyeongsang National University, Jinju 660-701, Republic of Korea*
[d] *Clinical Research Institute, Gyeongsang National University Hospital, Gyeongsang National University, Jinju 660-701, Republic of Korea*
[e] *Research Institute of Life Science, Gyeongsang National University, Jinju 660-701, Republic of Korea*
[f] *Animal Biotechnology Division, National Institute of Animal Science, Rural Development Administration, Suwon 441-706, Republic of Korea*

ARTICLE INFO

Article history:
Received 22 July 2011
Received in revised form
13 February 2012
Accepted 17 February 2012

Keywords:
Mesenchymal stem cells
Skin
Bone marrow
Dental follicle
Osteogenesis
Human

ABSTRACT

The present study evaluated the human mesenchymal stem cells (hMSCs) isolated from skin (hSMSC), bone marrow (hBMSC) and dental follicle (hDFMSC) tissues on their *in vitro* and *in vivo* osteogenic potential using demineralized bone matrix (DBM) and fibrin glue scaffold. Cells originated from three distinct tissues showed positive expressions of CD44, CD73, CD90, CD105 and vimentin, and differentiation ability into osteocytes, adipocytes and chondrocytes. hMSCs from all tissues co-cultured with a mixed DBM and fibrin glue scaffold in non-osteogenic induction media were positively stained by von Kossa and expressed osteoblast-related genes, such as osteocalcin (OC), osteonectin (ON), runt-related transcription factor 2 (Runx2) and osterix. For *in vivo* osteogenic evaluation, PKH26 labeled hMSCs were implanted into the subcutaneous spaces of athymic mice with a mixed scaffold. At 4 weeks of implantation, PKH26 labeled cells were detected in all hMSC-implanted groups. Bone formation with OC expression and radio-opacity intensity were observed around DBM scaffold in all hMSC-implanted groups. Interestingly, hDFMSCs-implanted group showed the highest OC expression and calcium content. These findings demonstrated that hDFMSCs could be a potential alternative autologous cell source for bone tissue engineering.

1. Introduction

Reconstruction of a large bone defect after trauma or bone surgery has been a great challenge in the clinical field. Autologous bone graft technique has been considered as a gold standard, but it has several serious disadvantages, such as unavailability in large defects and donor site complications (Arrington et al., 1996; Liu et al., 2008). Recently, bone regeneration by tissue engineering has been considered as a substitute for autologous bone graft technique (Jeon et al., 2008; Liu et al., 2008; Mauney et al., 2004, 2005; Petite et al., 2000; Yuan et al., 2007). Pluripotent and multipotent stem or precursor cells are the most essential elements in tissue engineering procedures. Although mesenchymal stem cells (MSCs) derived from bone marrow (BMSCs) have been most widely studied in *in vitro* and *in vivo* bone formations, attempts have been made to obtain stem cells with multilineage differentiation abilities from more easily accessible sources, such as skin, fat, oral periosteum and dental tissues (Gronthos et al., 2000; Kajahn et al., 2008; Lindroos et al., 2008; Morsczeck et al., 2005; Park et al., 2007; Riekstina et al., 2008, 2009).

In previous reports, skin stem cells were isolated from the floating sphere formed cells in serum-free specific culture conditions (Fernandes et al., 2008; Toma et al., 2001), and represented the characteristics of embryonic neural crest-derived precursor cells, known as skin-derived precursors. However, in skin, other putative stem cells were also reported, including skin-derived

Abbreviations: AP, alkaline phosphatase; ADMEM, advanced Dulbecco's modified Eagle medium; BMPs, bone morphogenic proteins; BMSCs, bone marrow-derived mesenchymal stem cells; CD, cluster of differentiation; CT, computed tomography; DAPI, 4′,6-diamino-2-phenylindole; DBM, demineralized bone matrix; DMEM, Dulbecco's modified Eagle medium; DPBS, Dulbecco's phosphate buffered saline; FBS, fetal bovine serum; FITC, fluorescein isothiocyanate; GAPDH, glyceraldehyde-3-phosphate dehydrogenase; hBMSCs, human bone marrow-derived mesenchymal stem cells; hDFMSCs, human dental follicle-derived mesenchymal stem cells; hMSCs, human mesenchymal stem cells; hSMSCs, human skin-derived mesenchymal stem cells; MSCs, mesenchymal stem cells; OC, osteocalcin; ON, osteonectin; RT-PCR, reverse transcription-polymerase chain reaction; Runx2, runt-related transcription factor 2; SMSCs, skin-derived mesenchymal stem cells

* Corresponding author at: OBS/Theriogenology and Biotechnology, College of Veterinary Medicine, Gyeongsang National University, 501 Jinju-daero, Jinju 660-701, Republic of Korea. Tel.: +82 55 772 2347; fax: +82 55 772 2349.
E-mail address: jinrho@gnu.ac.kr (G.-J. Rho).

0301-4681/$ - see front matter © 2012 International Society of Differentiation. Published by Elsevier B.V. All rights reserved.
Join the International Society for Differentiation (www.isdifferentiation.org)
doi:10.1016/j.diff.2012.02.008

MSCs (SMSCs) and epidermal stem cells, following different isolation and culture methods compared to those of skin-derived precursors (Kang et al., 2010; Riekstina et al., 2008, 2009). In addition, the dental tissues from extracted teeth may be used as potential autologous cell sources for the isolation of putative stem cells. The dental stem cells were firstly isolated from the dental pulp tissues of extracted third molars (Gronthos et al., 2000, 2002). Subsequently, other tissue sources for dental stem cells, such as periodontal ligament (Seo et al., 2004), root apical papilla (Reynolds and Jahoda, 2004), and dental follicle (Morsczeck et al., 2005, 2008) were also explored. Interestingly, the dental follicle-derived cells have shown the enhanced expression of osteoblast-specific transcription factors, osterix and runt-related transcription factor 2 (Runx2), after their osteogenic differentiation (Morsczeck et al., 2009). Moreover, MSC-like characteristics of dental stem cells with plastic adherent property, expression of cell surface specific markers and *in vitro* multilineage differentiation ability were similar to those of skin derived stem cells (Kang et al., 2010; Lindroos et al., 2008; Riekstina et al., 2009).

It is well known that the choice of a proper scaffold is another pivotal factor in bone tissue engineering field, which provide cell migration through the matrix and attachment. Although various biomaterials, including demineralized bone matrix (DBM) (Liu et al., 2008; Mauney et al., 2004, 2005; Schwarz et al., 1989; Yuan et al., 2007), β-tricalcium phosphate (Kasten et al., 2003; Yamada et al., 2003; Yuan et al., 2007), hydroxyapatite (Kasten et al., 2003), and other biodegradable materials (Perka et al., 2000) have been available, DBM has been widely used as a cell deliverer for *in vitro* and *in vivo* osteogenesis of stem cells. It possesses osteoinductive potential due to the presence of various growth factors, such as bone morphogenic proteins (BMPs) and extracellular proteins (Blum et al., 2004; Wildemann et al., 2007). Particularly, it has been reported that a range of BMPs in DBM, such as BMP-2, BMP-4, and BMP-7 plays a key role in osteoblast differentiation and directly induce bone formation *in vitro* and *in vivo* (Jeon et al., 2008; Pietrzak et al., 2006; Wildemann et al., 2007).

The objective of this study was to evaluate the osteogenic potential in human MSCs (hMSCs) isolated from different tissue sources to determine whether these tissues are worthy to preserve as autologous hMSC sources in future. We isolated hMSCs from three distinct human somatic tissues, such as skin, bone marrow and dental follicles of impacted teeth. After being characterized with adherent growth in culture dishes, expression of MSC-specific cell surface makers (CD44, CD73, CD90, CD105 and vimentin) and *in vitro* differentiation into osteocytes, adipocytes and chondrocytes in specific induction media, hMSCs of different origins were assessed for *in vitro* osteogenesis with DBM and fibrin glue scaffold in a non-osteogenic inductive media. Furthermore, *in vivo* osteogenesis of three types of hMSCs with the same scaffold was evaluated after 4 weeks of implantation into the subcutaneous spaces of athymic mice.

2. Materials and methods

2.1. Chemicals and media

All chemicals were purchased from Sigma chemical company (Sigma, St. Louis, MO, USA) and media from Gibco (Invitrogen, Burlington, ON, Canada), unless otherwise specified.

2.2. MSCs isolation from human skin, bone marrow and dental follicle tissues

All tissues used in the present study were collected and handled following the approval of Research Ethical Committee of the Gyeongsang National University Hospital, with informed consents of the patients for their tissue donations (GNUHIRB-2009-34). All animal experiments were authorized by the Animal Center for Medical Experimentation at Gyeongsang National University.

Human skin-derived MSCs (hSMSCs) were harvested from $1 \times 5\ cm^2$-sized elliptical skin samples obtained from four patients (22–29 years old, average 25 years) during head and neck surgery via the submandibular approach. After removing hairs and subcutaneous fat tissues, the epidermis and dermis of skin tissue were sliced into 1–3 mm^2 explants. The explants were attached onto a plate and cultured in 1 ml Dulbecco's Modified Eagle Medium (DMEM)/F12 (1:1) supplemented with 10% fetal bovine serum (FBS, Gibco), 10 ng/ml epidermal growth factor, 10 ng/ml basic fibroblast growth factor, 100 U/ml penicillin, and 100 μg/ml streptomycin at 37 °C in a humidified atmosphere containing 5% CO_2 in air for 3–5 days. After the removal of skin fragments, the attached cells were allowed to grow under similar culture conditions.

Human bone marrow-derived MSCs (hBMSCs) were harvested from marrow extracts obtained from the routine iliac bone graft procedure for the reconstruction of cleft alveolus and vertebral spine defects in four patients (18–45 years old, average 31 years). All bone marrow donors were generally healthy with no specific metabolic or inherited diseases. hBMSCs were isolated and expanded using a slightly modified method as previously reported (Liu et al., 2008; Mauney et al., 2005). Briefly, after the dilution of bone marrow aspirates with Dulbecco's phosphate buffered saline (DPBS) at a ratio of 1:2 (v/v), nucleated cells were isolated using a density gradient solution (Ficoll-Paque™ PLUS; 1.077 g/ml, GE Healthcare, Uppsala, Sweden). A total of 4 ml DPBS with bone marrow aspirate was layered onto 3 ml of Ficoll-Paque™ PLUS solution in a 15 ml conical tube and centrifuged at $400 \times g$ for 40 min. The interface buffy layer from the tube was collected, and washed twice in DPBS by centrifugation $500 \times g$ for 5 min. Nucleated cells were cultured at a density of 1×10^3 cells/cm^2.

Human dental follicle-derived MSCs (hDFMSCs) were harvested from the attached dental follicles separated from the calcified teeth after impacted third molars extractions in four orthodontic treatment patients (16–18 years old; average 17 years old). hDFMSCs were isolated and expanded using a slightly modified method as previously reported (Lindroos et al., 2008; Morsczeck et al., 2005). The separated dental follicle tissues were washed in DPBS 3 times and sliced into 1–3 mm^2. The sliced dental follicle tissues were digested in a solution of 0.1 U/ml collagenase type I for 15 min, followed by mechanical dissociation with vigorous pipetting, and were centrifuged at $500 \times g$ for 5 min in DPBS. To remove cell clumps and debris cells, the suspended cells were passed through a 40 μm nylon cell strainer (BD Falcon™, BD Biosciences, Franklin Lakes, NJ, USA). After being centrifuged at $500 \times g$ for 5 min, dental follicle cells were allowed for culture.

Once confluent, all three types of hMSCs were dissociated using a 0.25% (w/v) trypsin-EDTA (Gibco) and made into pellets by centrifugation at $500 \times g$ for 5 min. Cells were then re-grown in advanced Dulbecco's modified eagle's medium (ADMEM) supplemented with 10% FBS, 100 U/ml penicillin, and 100 μg/ml streptomycin at 37 °C in a humidified atmosphere of 5% CO_2 in air by changing culture medium twice a week and passaged three times for further analysis.

2.3. Characterization of MSCs derived from human skin, bone marrow, and dental follicle tissues

hMSCs at passage 3 were analyzed for the expression of surface and intracellular markers by a flow cytometer (BD FACSCalibur; Becton Dickinson and Company, Franklin Lakes, NJ,

USA) in triplicates. After being harvested using 0.25% trypsin-EDTA solution, hMSCs were fixed in 3.7% formaldehyde solution and labeled directly with fluorescein isothiocyanate (FITC)-conjugated antibodies [anti-mouse CD44 (1:100; BD Pharmingen™, BD Biosciences, Franklin Lake, NJ, USA), anti-human CD90 (1:100; BD Pharmingen™), and CA, USA] or with unconjugated primary antibodies [anti-human CD73 (1:100; BD Pharmingen™), anti-mouse CD105 and anti-mouse CD45 (1:100, Santa Cruz biotechnology, Inc., CA, USA)]. To evaluate the expression of vimentin, cells were incubated in ice cold methanol for fixation and permeabilization. Then, the primary antibody [mouse anti-vimentin (1:100; Sigma-Aldrich)] and FITC-conjugated secondary antibody [goat anti-mouse Ig G (1:100; BD Pharmingen™)] were sequentially applied to hMSCs

In vitro differentiation of each hMSCs at passage 3 were induced into osteogenic, adipogenic and chondrogenic lineages by culturing under suitable conditions for 21 days by following previously described methods (Jeon et al., 2011; Park et al., 2012). Media were changed twice a week. Osteogenic medium consisted of DMEM supplemented with 0.1 μM dexamethasone, 50 μM ascorbate-2-phosphate and 10 mM glycerol-2-phosphate. Adipogenic medium was consisted of DMEM supplemented with 1 μM dexamethasone, 10 μM insulin, 100 μM indomethacin and 500 μM isobutylmethylxanthine. Chondrogenic differentiation was induced in chondrogenic medium (HyClone Advance STEM™, Thermo Fisher Scientific Inc., Waltham, MA, USA).

Differentiated cells were evaluated by von Kossa, Oil red O and alcian blue 8GX staining to confirm the formation of osteocytes, adipocytes and chondrocytes, respectively, by following previously described protocols (Jeon et al., 2011; Kang et al., 2010; Ock et al., 2010).

2.4. *In vitro* osteogenesis of hMSCs with a mixed DBM and fibrin glue scaffold

A total of 1×10^6 cells of each three distinct hMSCs mixed with 0.3 ml of fibrin glue (Greenplast® kit, Green Cross, Yongin, Korea) was injected and simultaneously coated into a quarter ($0.4 \times 0.8 \times 0.4$ cm^3-size) of DBM scaffold (Grafton®, Osteotech™, Eatontown, NJ). The hMSCs seeded scaffolds were incubated in DMEM with 10% FBS at 37 °C in a humidified atmosphere of 5% CO_2 in air by changing the culture medium twice a week. After 2 and 4 weeks of incubation, the cells and scaffolds were fixed in 3.7% (w/v) formaldehyde solution and evaluated for *in vitro* osteogenesis using von Kossa, alizarin red and alkaline phosphatase (AP) staining as described previously (Jeon et al., 2011; Kang et al., 2010; Ock et al., 2010).

The *in vitro* co-cultured cells were collected with cell strainer (BD Falcon™) for the isolation of total RNA (Kang et al., 2010). The relative mRNA abundance of osteocalcin (OC), osteonectin (ON) Runx2 and osterix as bone and osteoblast-related markers of hMSCs co-cultured in the mixed scaffold was analyzed using reverse transcription polymerase chain reaction (RT-PCR). Primers used for amplification are summarized in Table 1. Total RNA isolation, cDNA synthesis and RT-PCR amplification methods were carried out as previously described (Kang et al., 2010): pre-denaturation at 94 °C for 3 min, followed by 34 cycles of denaturation at 94 °C for 45 s, annealing at 60 °C (OC and ON) or 56 °C (Runx2 and osterix) for 30 s, elongation at 72 °C for 45 s, and a final elongation at 72 °C for 10 min. These PCR products were loaded on 1% agarose gel electrophoresis with 0.1 μg/mL ethidium bromide (Gibco). For the gene expression levels, densitometric semiquantitative RT-PCR analysis was performed as described previously (Ock et al., 2010). Briefly, RT-PCR expression level for each gene was normalized to glyceraldehyde-3-phosphate dehydrogenase (GAPDH) mRNA levels and presented as a fold induction with mean ± standard deviation (SD). Relative intensities of each specific band were calculated on the basis of GAPDH intensity by GelViewer Version 1.5 (CURVEX Corp., Korea). A minimum of three replicates were used for statistical analysis.

2.5. *In vivo* osteogenesis of hMSCs with a scaffold in athymic mice

On the previous day of cell seeding in DBM for *in vivo* transplantation, hMSCs at 70% confluence were labeled with a fluorescent lipophilic carbocyaninine dye, PKH26 by following a method described previously (Kang et al., 2010; Park et al., 2012).

A total of 1×10^6 cells from each hMSCs labeled with PKH26 mixed with 0.3 ml of fibrin glue was injected and simultaneously coated into a DBM scaffold (a quarter of 0.5 cm^3 Grafton-Block, $0.4 \times 0.8 \times 0.4$ cm^3-size). A mixture of each hMSCs and scaffold was implanted under the skins of 4 athymic nude mice (8-week-old males, Charles River, Orient Bio Inc., Sungnam, Korea). Under general anesthesia with subcutaneous injection of a combination of 0.5 μl/g of tiletamine–zolazepam (Zoletil®, Virbac, Carros, France) and 0.5 μl/g xylazine (Rompun®, Bayer Korea Ltd., Seoul, Korea), small skin incisions were made and four subcutaneous pouches per mouse were formed in the back of experimental animals. The scaffold mixtures injected with hSMSCs, hBMSCs and hDFMSCs were sequentially implanted into the subcutaneous pouches. The non-cell seeded scaffold mixture as a control was also implanted into the last subcuticular pouch. After the completion of four implantations per one mouse, the skin incisions were closed with 4–0 nylons.

Table 1
Primers used for evaluating *in vitro* osteogenesis by RT-PCR.

Gene	Sequence of primer (5′–3′)	Product size (bp)	Annealing Tm (°C)	Accession number
GAPDH[a]	F-GAGTCAACGGATTTGGTCGT R-TTGATTTTGGAGGGATCTCG	238	60	AB062273
Osteocalcin (OC)	F-CCCCGCTTCCTCTTTAGACT R-GCCAACCCCAAAGGATATT	231	60	AY147065
Osteonectin (ON)	F-GTGCAGAGGAAACCGAAGAG R-AAGTGGCAGGAAGAGTCGAA	202	60	NM_003118
Runx2[b]	F-CCTTGGGAAAAATTCAAGCA R-AACACATGACCCAGTGCAAA	181	56	NM_001015051
Osterix	F-GCAGCTAGAAGGGAGTGGTG R-GCAGGCAGGTGAACTTCTTC	359	56	NM_152860

[a] Glyceraldehyde-3-phosphate dehydrogenase.
[b] Runt-related transcription factor 2.

2.6. Radiological and histological analyses of in vivo transplants

Animals were euthanized at 4 weeks after implantations to evaluate their calcification with plain radiographs and computed tomography (CT, SOMATOM Emotion 6, Siemens, Munich, Germany). The CT images of implantation sites were analyzed and compared by intensity analyzing software (Syngo CT 2004A, Siemens). After obtaining radiographs, the implanted subcutaneous tissues were harvested *en bloc*, and the specimens were carefully divided into longitudinal sections for histological studies and fluorescence observation.

One of the sectioned specimens from each implanted tissues was used for observation of PKH26-positive cells. Briefly, tissues were embedded in optimal cutting temperature compound (Tissue-Tek®, Sakura Finetechnical Co., Ltd., Tokyo, Japan), and rapidly frozen at −23 °C and cut into 4 μm sections using Cryocut equipment (LEICA CM3050S, Leica, Wetzlar, Germany). The sections were mounted on glass slides and counterstained with 4′,6-diamino-2-phenylindole (DAPI, Vectasheid®, Vector Lab, Burlingame, CA). Fluorescent expression was assessed by a fluorescence microscope (BX51, Olympus, Tokyo, Japan) using a fluorescent digital camera (DP72, Olympus). The number of cells expressing DAPI and PKH26 was determined using microscope photography, and the ratio of PKH26 positive cells to DAPI expressing cells was calculated in each hMSCs grafted specimens. A minimum of four glass slides of each grafted groups were evaluated.

The other specimens of each implantation were fixed with 10% neutral buffered formalin for 24 h, embedded in a paraffin block, cut into 4 μm section, and mounted on the silane-coated slides. The sections were maintained at room temperature for 12 h and deparaffinized. Hematoxylin and eosin staining was followed after hydration. Total observed cells were counted and calculated per cm^2. A minimum of four sections per each group were evaluated. Immunohistochemical staining for OC was conducted using an automated immunostainer (LabVision Autostainer™; LabVision, Thermo Fisher Scientific Inc., Fremont, CA). Deparaffinization and antigen retrieval of specimens were performed simultaneously using Tris-EDTA buffer (LabVision). Glass slides were incubated in a PTmodule™ (LabVision) at 100 °C for 25 min, washed with Tris-buffered saline (LabVision) twice (3 min each time), and treated with hydrogen peroxide at room temperature for 10 min. The sections were exposed to primary mouse monoclonal anti-OC antibody (ab13418, Abcam, Cambridge, UK, 1:200) at room temperature for 40 min, treated with a biotinylated polyvalent secondary antibody solution, incubated with a horseradish peroxidase-conjugated avidin-biotin complex, and treated with 3,3-diaminobenzidine and hydrogen peroxidase. Finally, the nuclei were counterstained with hematoxylin. Densitometric analyses of *in vivo* OC expressions were performed using analySIS TS™ software (Olympus Soft Imaging Solution, Münster, Germany) after the selection of minimum 4 slides of each implantation sites.

2.7. Measurement of calcium content in in vivo implanted specimens

To measure the calcium contents of *in vivo* implanted specimens, each sample was deparaffinized, dried at 95 °C for 1 h, weighed, and decalcified in 1 ml of Calci-Clear Rapid (National Diagnostics, Atlanta, GA). The calcium content of the supernatants was determined by spectrophotometry using Methylxylene blue method (Calcium E-test Wako, Wako Pure Chemical Industries, Osaka, Japan) according to the manufacturer's instructions. The calcium levels of each group were expressed as mean ($n=3$) of nanogram (ng) of calcium per milligram (mg) of cell and scaffold specimen.

2.8. Statistical analysis

All values were statistically analyzed by one-way analysis of variance (ANOVA) and independent group variables were compared using Tukey's multiple comparisons and Bonferroni tests. Data were expressed as mean ± SD, and their differences were considered to be significant when $p < 0.05$.

3. Results

3.1. General characteristics of hMSCs

Isolated and cultured hMSCs from three different tissue sources showed similar growth patterns with homogenous fibroblast-like appearance and grown as adherent cells in culture dishes. All three types of cells in the present study revealed the expression of MSC specific markers, such as CD44, CD73, CD90, CD105 and vimentin by FACS analysis as shown in Fig. 1. However, CD45, a marker of hematopoietic cells was relatively low in all hMSCs. In addition, all

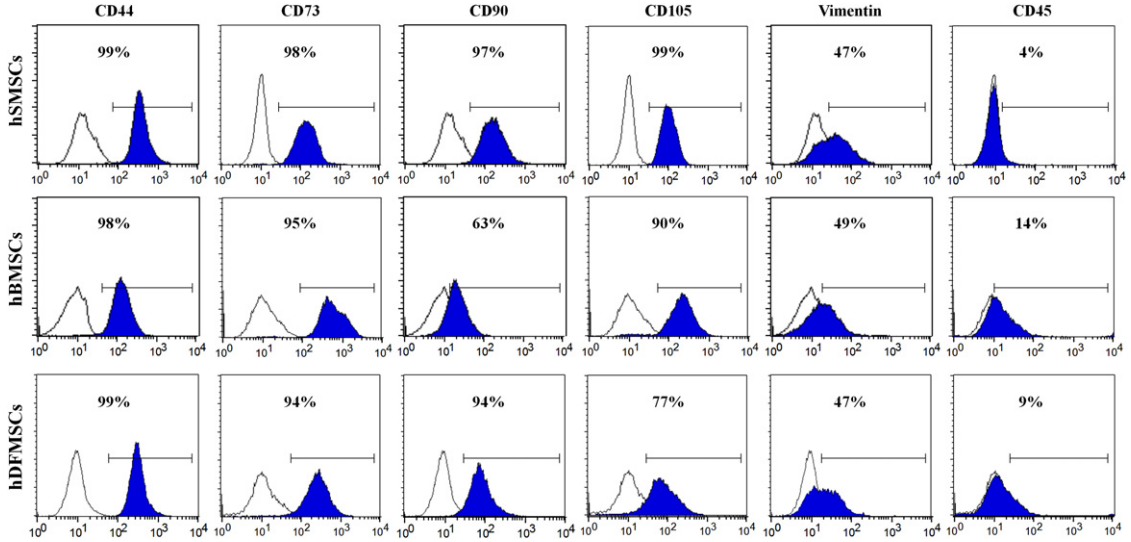

Fig. 1. Fluorescence activated cell sorting (FACS) analysis of three kinds of hMSCs originated from skin, bone marrow, and dental follicle. All hMSCs at third passage were positive for MSC specific markers (CD44, CD73, CD90, CD105, vimentin). Moreover, a relatively low level of expression was observed for a marker of hematopoietic cells (CD45). An open area indicates an antibody isotype control and a shaded area represents specific marker antibodies.

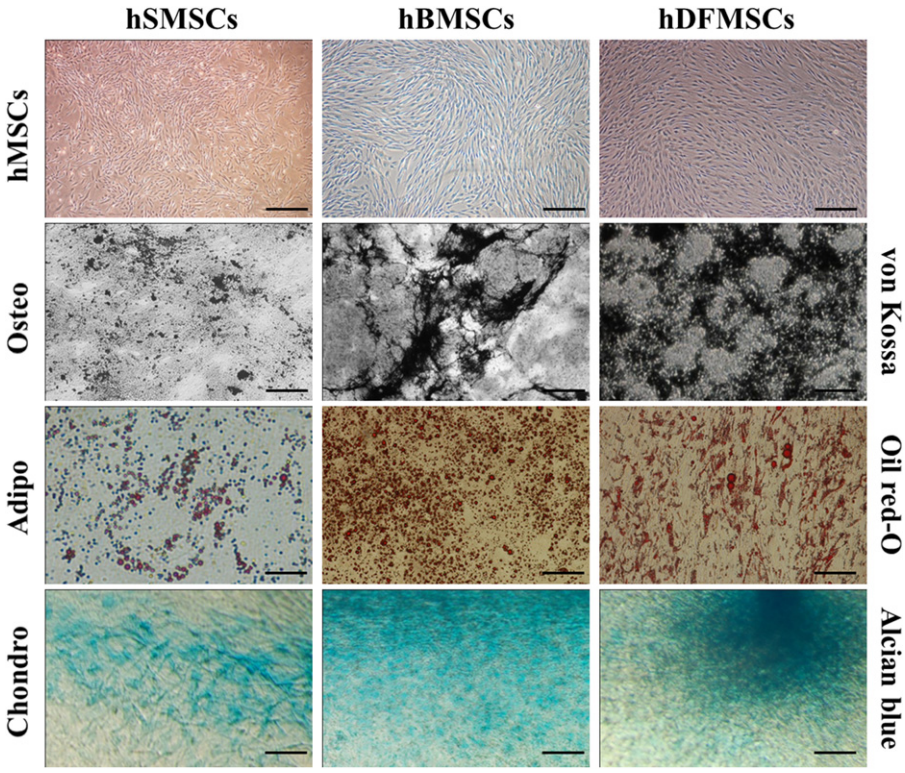

Fig. 2. Characterization and *in vitro* differentiation of hMSCs. Cultured hMSCs from three different sources showed similar growth characteristics with plate adherence and fibroblast-like morphology at passage 2. Although all hMSCs showed successful osteogenic (Osteo), adipogenic (Adipo) and chondrogenic (Chondro) differentiation, hBMSCs and hDFMSCs exhibited enhanced staining intensities for the differentiation into mesenchymal lineages (Osteo, Adipo and Chondro) than hSMSCs. Scale bar = 100 μm.

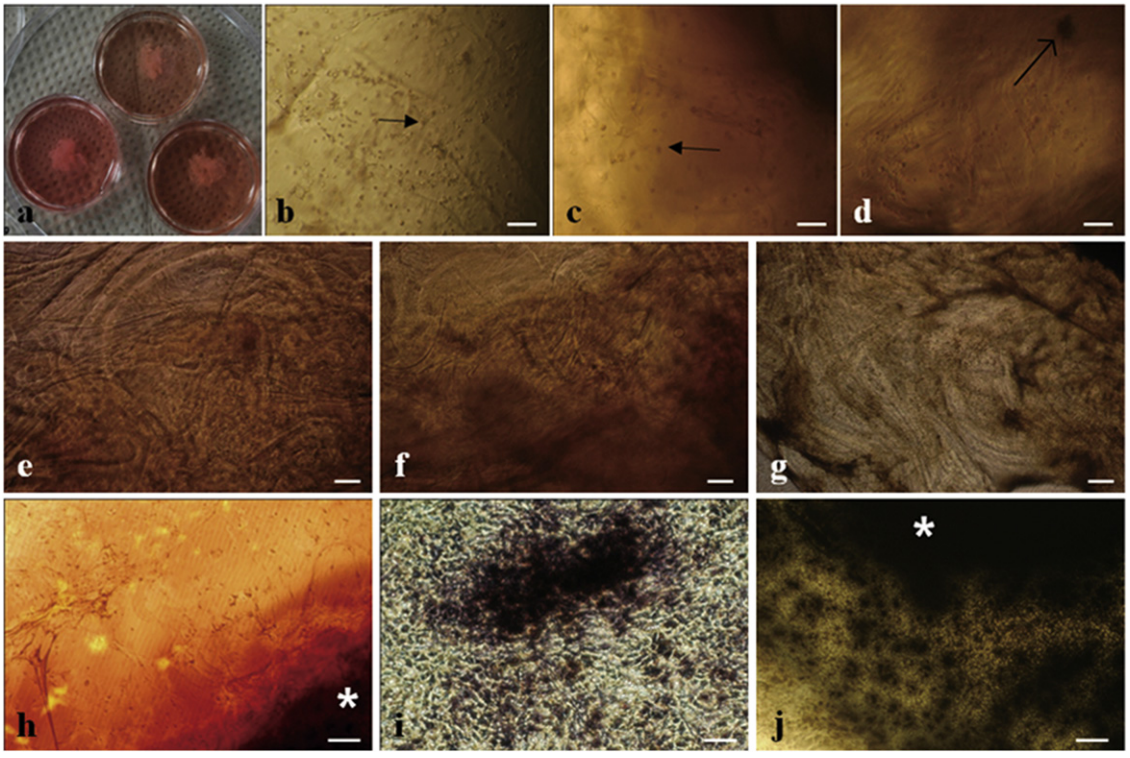

Fig. 3. *In vitro* co-cultures of hMSCs with a mixed demineralized bone matrix (DBM) and fibrin glue scaffold in non-osteogenic inductive media. (a) Macrographic image on first day of co-cultures. (b–j) Similar *in vitro* osteogenic reactions were observed in three different kinds of co-cultured hMSCs (b, e, h: hSMSCs; c, f, i: hBMSCs; d, g, j: hDFMSCs). (b) Numerous homogenous shaped and plate-adherent hSMSCs (arrow) were clearly observed after one week of co-culture (c and d). As culture time passed to 2 (c) and 4 (d) weeks, seeded hMSCs (arrow) were more stably attached to culture plate and DBM scaffold. At this time point, dark brown mineral depositions (open arrow) were also observed in the culture plate (e–g). At 4 weeks of co-culture, all types of hMSCs showed similar appearances with unclear margins of DBM scaffold, which were possibly related to newly-generated bone minerals in culture media. In addition, three types of hMSCs were successfully stained with alizarin red (h), alkaline phosphatase (i), and von Kossa (j) staining ('*' is showing the periphery of DBM scaffold). Scale bar = 50 μm.

three types of hMSCs were successfully differentiated *in vitro* into osteocytes, adipocytes and chondrocytes following induction in specific media. However, hBMSCs and hDFMSCs showed enhanced staining intensities for the differentiation into mesenchymal lineages, including osteocytes, adipocytes and chondrocytes (Fig. 2). These findings demonstrated that the cells from three different sources, such as skin, bone marrow and dental follicle tissues, had possessed the characteristics of MSCs.

3.2. *In vitro* osteogenesis of hMSCs

In vitro osteogenesis of porcine SMSCs, co-cultured with DBM and fibrin glue scaffold in a non-osteogenic medium was observed in our previous study (Kang et al., 2010). In this study, a similar and successful *in vitro* osteogenesis was observed in all types of hMSCs with the same scaffold and culture conditions. During the first two weeks after hMSCs seeding in the DBM and fibrin glue scaffold, cells exhibited homogenous and plate adherent growth in the periphery and interior of scaffold (Fig. 3b, c). As *in vitro* co-culture time progressed to 2 and 4 weeks, the similar characteristics, including unclear margins of DBM due to dark brown depositions, which were certainly related to newly-generated bone minerals around seeded cells into DBM scaffold, were observed in all kinds of hMSCs co-culture groups (Fig. 3d–g). Moreover, mineralized matrix in each hMSCs was identified by bone specific staining, alizarin red, AP and von Kossa, after 4 weeks of co-culture with the scaffold (Fig. 3h–j).

By RT-PCR, the expressions of OC, ON Runx2 and osterix were detected in *in vitro* co-cultured hMSCs with DBM and fibrin scaffold at 2 and 4 weeks of culture (Fig. 4a). The relative mRNA levels of bone and osteoblast-related genes, OC, ON Runx2 and osterix, in co-cultured cells varied at different time points of 2 and 4 weeks (Fig. 4b–e). In undifferentiated hMSCs (Day 0), OC expression was barely detected, and ON, Runx2 and osterix were expressed at relatively lower levels. However, their relative expression levels were enhanced by co-culturing with DBM and fibrin scaffold. In hSMSCs co-cultured group, extracellular matrix glycoproteins, OC

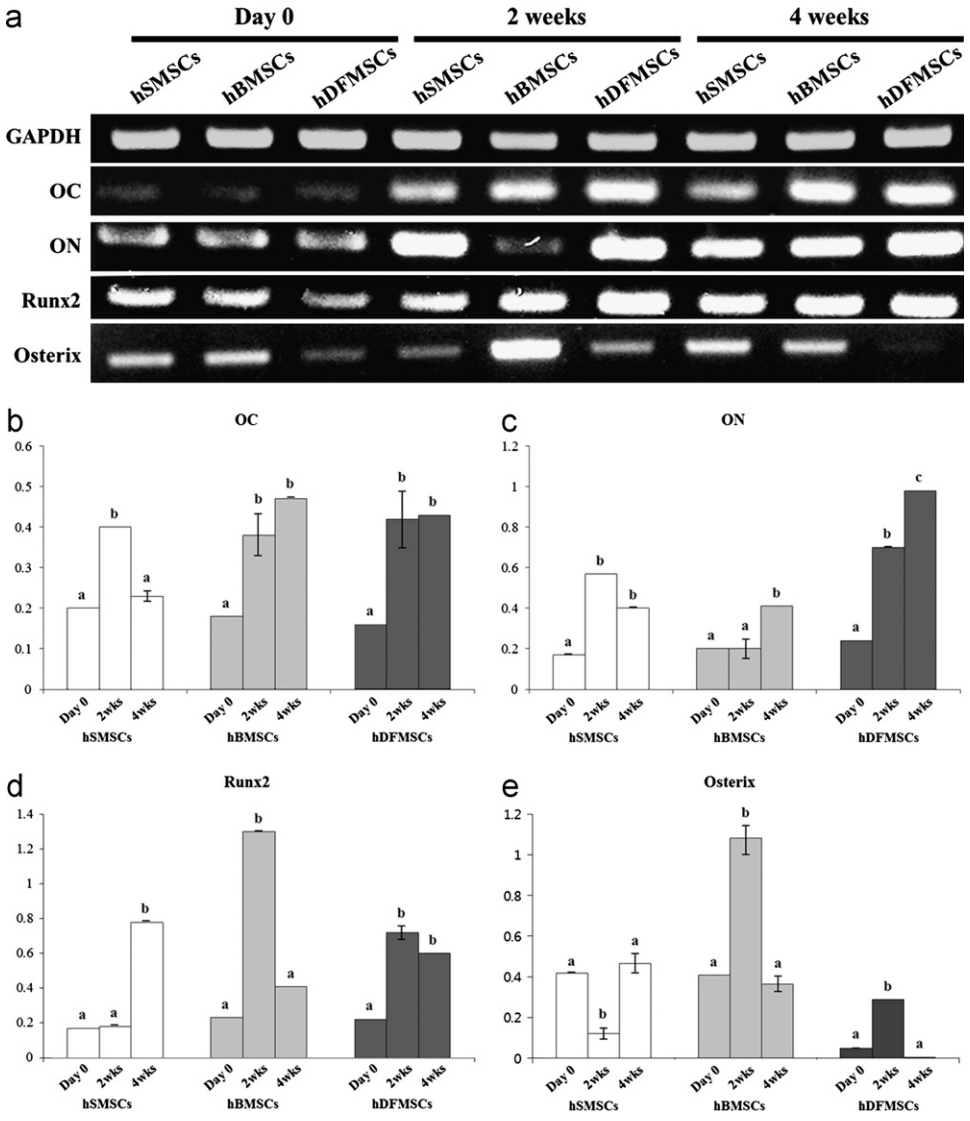

Fig. 4. Expression of osteocalcin (OC), osteonectin (ON), Runx2 and osterix in *in vitro* co-cultured hMSCs with a mixed DBM and fibrin glue scaffold by reverse transcription-polymerase chain reaction (RT-PCR) analysis. (a) In all co-cultured hMSCs, selected bone and osteoblast-related transcripts (OC, ON, Runx2 and osterix) were detected at 2 and 4 weeks of incubation. At Day 0, OC expression was barely detected, and ON, Runx2 and osterix were expressed at relatively low levels. The relative abundance of mRNA for OC (b), ON (c), Runx2 (d) and osterix (e) is shown during the co-culture period by semiquantitative RT-PCR analysis. In hSMSCs group, OC and ON were highly expressed at 2 weeks than at 4 weeks of culture, whereas Runx2 was higher at 4 weeks of cultured cells. However, in hBMSCs and hDFMSCs groups, OC and ON were expressed higher at 4 weeks than at 2 weeks of culture, but Runx2 and osterix were detected at higher level at 2 weeks of culture. Data represent the mean ± SD of three independent experiments, and different superscripts (a, b, c) indicate significant differences ($p < 0.05$).

and ON were expressed at higher levels at 2 weeks and decreased at 4 weeks of culture. However, the expression of osteoblast transcriptional factor, Runx2, was significantly higher in hSMSCs cultured for 4 weeks than for 2 weeks. Osterix, another important transcription factor essential for osteoblast differentiation, was also detected in hSMSCs co-cultured group, but its expression did not reach significantly ($p > 0.05$) higher levels after stimulation for 4 weeks. In contrast, hBMSCs and hDFMSCs groups expressed higher levels of OC and ON at 4 weeks culture, whereas Runx2 and osterix were detected at higher levels at 2 weeks.

3.3. *In vivo osteogenesis of hMSCs*

At 4 weeks after *in vivo* implantations, radiologic opacities were observed in the subcutaneous tissues of experimental athymic nude mice by plain and CT images (Fig. 5a, b). The intensity analysis of axial CT images showed that all hMSCs-transplanted groups had enhanced radiologic intensities than non-cell transplanted control group (Fig. 5c). However, hSMSCs implanted group showed no significant increase when compared with control.

By histological examination, the red fluorescent expressions of PKH26 were detected in all three hMSCs grafts (Fig. 6), indicating that *in vivo* grafted hMSCs were well-preserved and proliferated in the subcutaneous spaces of nude mice. The ratio of PKH26 positive cells to all observed cells (DAPI positive-cells) was slightly higher in hBMSC groups, but did not differ significantly ($p > 0.05$) among other hMSCs grafted groups (0.655 ± 0.103, 0.71 ± 0.096 and 0.694 ± 0.112 in hSMSC, hBMSC and hDFMSC, respectively).

Following optical microscopy with hematoxylin and eosin staining, all *in vivo* implanted materials were found to be well preserved in the subcutaneous tissues, and enhanced cell numbers were observed in hMSC grafted group than in control (Fig. 7A). At higher magnification of hMSC grafted groups, newly generated trabecular bones and its lining osteoblasts were observed between DBM scaffolds. Especially in hBMSCs and hDFMSCs grafted groups, newly generated vascular vessels and immature fibroblast-like cells (putative pre-osteoblasts) were considerably detected in the interstitial tissues between bone matrices (Fig. 7A). Further, at higher magnification images, PKH26 positive transplanted cells were detected not only in the DBM lining osteoblasts, but also in the osteocytes trapped at the inner space of newly generated bone matrix (Fig. 7B).

Immunohistochemical analysis for OC in each transplanted group showed stronger activities in hMSCs-implanted groups (Fig. 8a–f) than that of control groups (Fig. 8g, h). At higher magnification, the OC activities were strongly detected in the cellular components of *in vivo* osteogenesis specimens, such as bone matrix lining osteoblasts, immature fibroblast-like cells in the interstitial tissues, and entrapped osteocytes in the newly generated bones (Fig. 8b, d, f). However, in control specimens, newly generated bone or OC expression was barely observed around the graft material (Fig. 8g, h).

Cell numbers of each transplanted groups were counted under higher magnification of the hematoxylin and eosin stained specimens, and the highest counted cell number was detected in hBMSCs [72.62 ± 9.50 ($\times 10^4/cm^2$)] and hDFMSCs [63.67 ± 16.2 ($\times 10^4/cm^2$)] grafted groups. hSMSC-graft group [33.67 ± 1.53 ($\times 10^4/cm^2$)] also had increased cell numbers than control group [7.67 ± 2.08 ($\times 10^4/cm^2$)], but lower than other two hMSCs grafted groups (Fig. 9a). The result of image analysis for *in vivo* OC expression revealed the highest intensity in hDFMSCs grafted specimen, but there was no statistical difference between three kinds of hMSCs (Fig. 9b). The total calcium content of *in vivo* specimens was calculated as ng per mg of tissue samples (ng/mg), and the observed values for hSMSCs, hBMSCs, hDFMSCs and control were 51.8 ± 4.1, 38.8 ± 3.8, 146.7 ± 8.1, and 22.3 ± 5.8, respectively (Fig. 9c). All hMSCs grafted specimens showed significantly ($p < 0.05$) higher calcium content than control specimen. Among hMSCs groups, no difference was observed between hSMSCs and hBMSCs, whereas hDFMSCs showed significantly higher calcium content than other types of hMSCs.

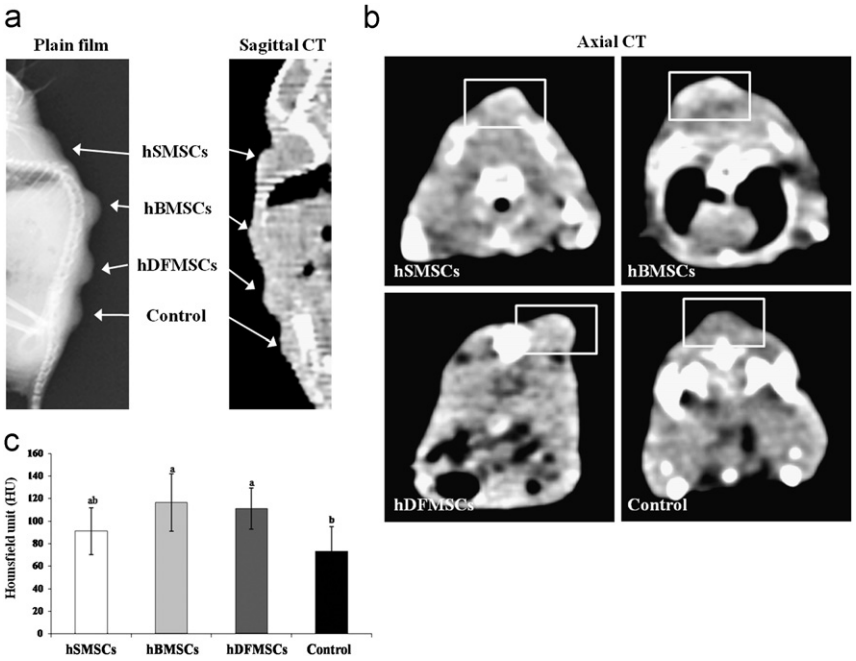

Fig. 5. Radiologic analysis of *in vivo* osteogenesis of hMSCs implanted with a DBM and fibrin scaffold into the subcutaneous tissues of athymic nude mice. (a) Using plain radiography and sagittal computed tomography (CT), implanted materials were obviously detected in the back subcutaneous tissues. (b) Axial CT views showed more enhanced radiologic intensities in all types of hMSCs implanted groups than in control group. (c) The radiologic intensities of implanted sites. All hMSCs grafted groups showed enhanced radiologic intensities compared to control group. Only hSMSCs grafted group showed no statistical difference in radiologic intensity with control. Data represent the mean ± SD of three independent experiments, and different superscripts (a, b) indicate significant differences ($p < 0.05$).

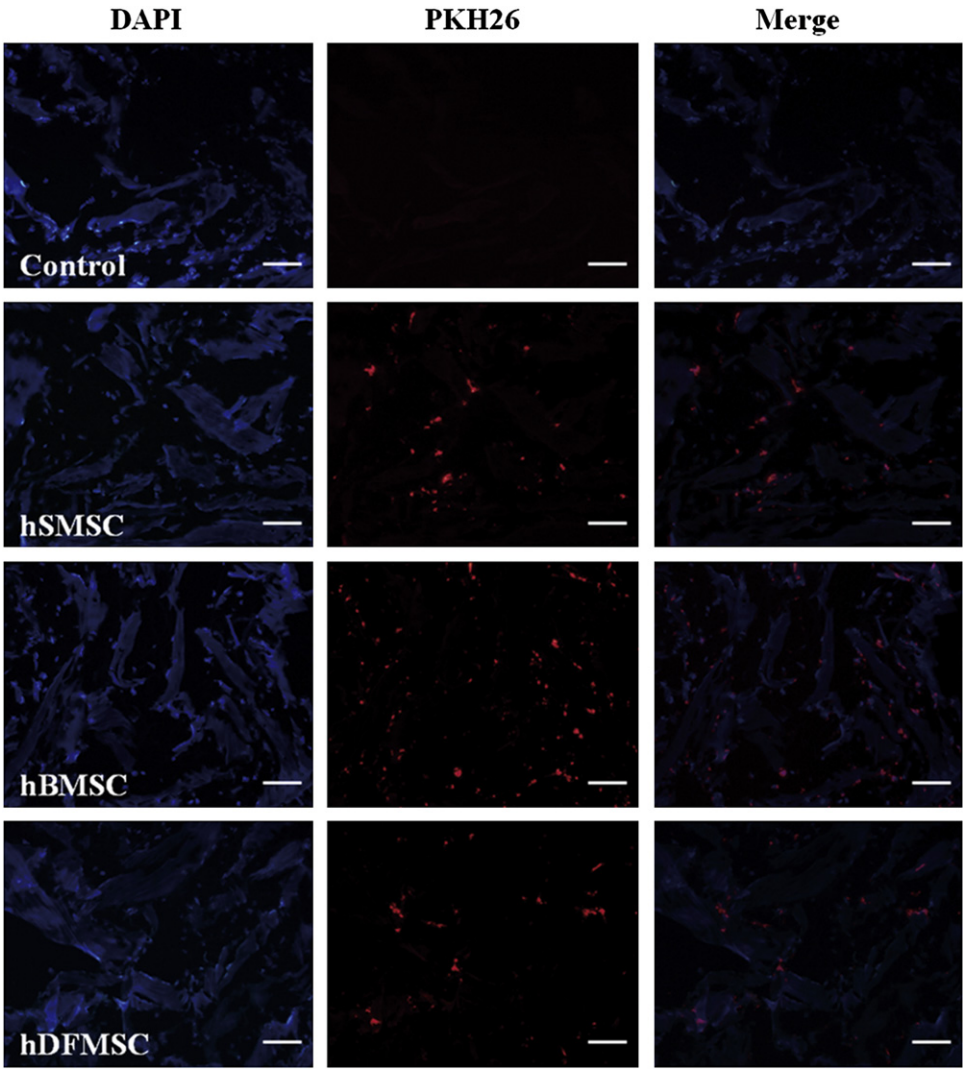

Fig. 6. Fluorescent expression of DAPI and PKH26, and their merged images in *in vivo* specimens of osteogenesis at 4 weeks after hMSCs grafts. Cells with PKH26 expression were positively detected between DBM scaffolds in all hMSCs implanted groups, but not in control group. Scale bar = 100 μm.

4. Discussion

In the present study, cells with MSC-like characteristics were isolated from three distinct human somatic tissues, and their *in vitro* and *in vivo* osteogenic potentials with a DBM scaffold were compared. A characteristic property of adherence to plastic culture dishes was employed to isolate hMSCs from skin, bone marrow and dental follicle tissues. No variability was observed in cultures prepared from different tissue sources. Isolated cells exhibited plastic adherent fibroblast-like cell growth, and positively expressed MSC specific markers (CD44, CD73, CD90, CD105 and vimentin). Interestingly, a small fraction of hMSCs was also detected for the expression of hematopoietic cell lineage marker, CD45. Among the three types of hMSCs, hBMSCs possessed a relatively higher population of CD45-positive cells followed by hDFMSCs and hSMSCs. Contrasting to a distinguishable property of MSCs with CD45-negative status, an earlier report suggested the presence of CD45-positive multipotential cells which were distinct from both hematopoietic cells and mesenchymal cells (Rogers et al., 2007). The findings of other studies further supported the existence of a subpopulation of CD45-positive cells in MSCs derived from bone marrow and the decidua of human term placenta (Kaiser et al., 2007; Kanematsu et al., 2011). These observations suggest that isolated hBMSCs and hDFMSCs in this study may represent a heterogeneous population comprised with the fractions of early progenitors, precursors and mature cells with MSC-like characteristics. However, studies on the multipotential properties of these individual cell types need to be further investigated. Besides these phenotypic properties, all hMSCs were successfully differentiated *in vitro* into osteocytes, adipocytes and chondrocytes under specific culture conditions. Even though slightly higher CD45-positive cells and differentiation ability were associated with hBMSCs and hDFMSCs, all three types of cells showed characteristic properties of MSCs that have been well demonstrated by previous reports (Gimble et al., 2008; Phinney and Prockop, 2007).

Following 4 weeks of *in vitro* co-culture of three kinds of hMSCs with DBM and fibrin glue scaffold in non-osteogenic inductive medium, AP, alizarin red and von-Kossa positive bone matrices were observed. Moreover, bone related extracellular matrix glycoproteins (OC and ON) and osteoblast-specific transcription factors (Runx2 and osterix) were detected in all hMSCs co-cultured with a mixed DBM and fibrin scaffold at 2 and 4 weeks of culture. Interestingly, in hSMSCs, OC and ON were highly expressed at 2 weeks of culture, whereas Runx2 was higher at 4 weeks of culture. Expression of osterix, although reduced at 2 weeks of culture, did not increase considerably after 4 weeks of induction. We also observed a similar pattern of expressions in

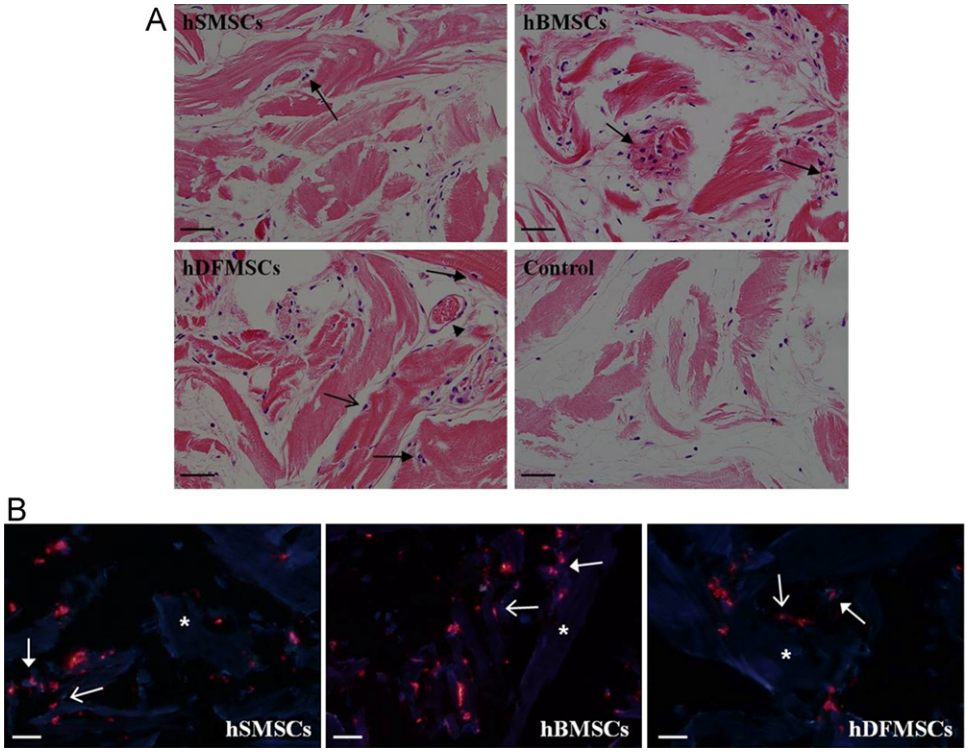

Fig. 7. Histologic features of *in vivo* implantations of hMSCs with DBM and fibrin glue scaffold at 4 weeks ((A) hematoxylin and eosin staining; (B) higher magnification of PKH26 expression in the *in vivo* specimens; scale bar=50 μm). (A) New bone regenerative activities and detectable cell numbers were enhanced in hMSC grafted groups than in control: immature fibroblast-like cells (putative pre-osteoblasts) around newly generated bone matrices (closed arrows in hSMSC and hBMSC specimens), DBM lining osteoblasts (open arrows), and osteocytes trapped in the newly generated bone spicules (closed arrows) were detected in all hMSCs implanted tissues. (B) Expression of PKH26 is shown at higher magnification of hMSCs grafts. PKH26 positive transplanted cells were detected not only in the DBM lining osteoblasts (open arrow), but also in the osteocytes trapped at the inner space of newly generated bone matrices (closed arrow) (*: grafted DBM scaffold; closed arrows indicate newly generated bones and trapped osteocytes; open arrows indicate DBM lining osteoblasts).

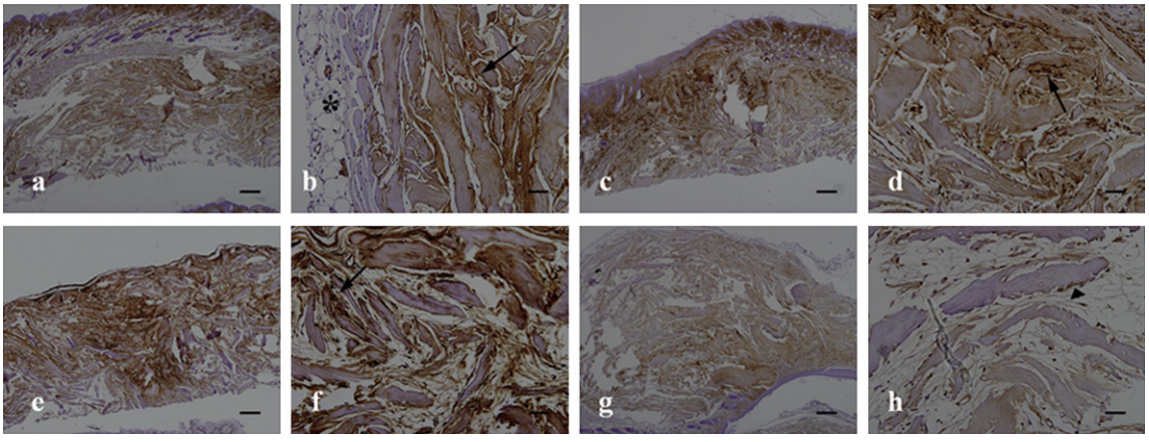

Fig. 8. Immunohistochemical expression of osteocalcin (OC) in *in vivo* implanted specimens (a, b: hSMSCs; c, d: hBMSCs; e, f: hDFMSCs; g, h: control; scale bar=a, c, e, g: 1000 μm; b, d, f, h: 50 μm). (a, c, e, g). In lower magnification of each implanted groups, higher expression level of osteocalcin was observed in hMSCs-grafted groups than in control (b, d, f). In higher magnification of hMSCs-grafted specimens, implanted materials were well-preserved under the subcutaneous fat and muscular tissues (*) and strong expression of OC in osteoblasts lining matrix bones (arrows) was detected in all hMSCs grafted groups. (h) Although the intensity and frequency were lower than hMSCs-grafted group, OC-positive lining osteoblasts around DBM scaffold were also detected in control specimen (arrowhead).

in vitro co-culture of porcine SMSCs with a DBM scaffold (Kang et al., 2010). In contrast to hSMSCs, hBMSCs and hDFMSCs groups showed higher levels of Runx2 and osterix at 2 weeks of induction, but lesser expression of OC and ON at 2 weeks than at 4 weeks of culture indicating an early initiation of osteoblast-differentiation. These observations suggest that the osteogenic differentiation of hMSCs from various origins may be affected by different regulation or cascade mechanisms in DBM scaffold, as it has been known to retain matrix incorporated osteogenic factors responsible for stimulation (Liu et al., 2008, 2010). Further, the differences in expression levels of marker genes could be related to the variability in osteogenic differentiation potential of hMSCs as exhibited under osteo-inductive conditions.

In addition to *in vitro* osteogenesis of hMSCs, successful *in vivo* bone formations were detected in the subcutaneous spaces of athymic mouse after transplantation of hMSCs, which were seeded in DBM scaffold. Our observations were in contrast to other previous studies, which had used either osteogenic differentiated cells from

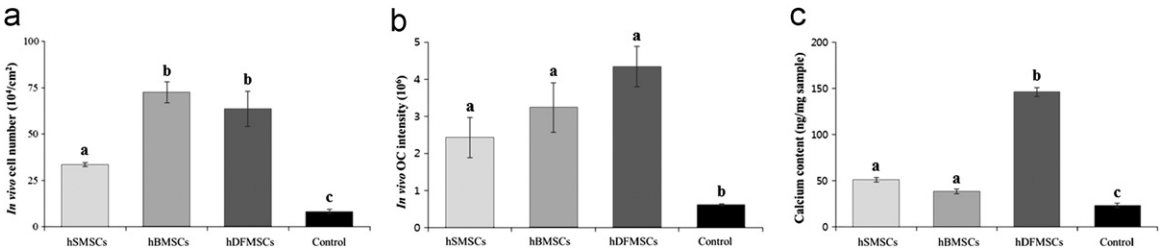

Fig. 9. Cell number, osteocalcin (OC) intensity and calcium content in *in vivo* osteogenesis specimens. (a) The cell numbers of hMSCs implanted groups were higher than that of control group. Among hMSCs, more increased cell number was found in hBMSCs and hDFMSCs grafted groups than in hSMSCs grafted group. (b) The intensity of *in vivo* OC expression and (c) calcium content were more enhanced in hMSCs-grafted groups than in control. Especially, hDFMSCs implanted group showed the highest *in vivo* OC intensity and calcium content. Data represent the mean ± SD of minimal three independent experiments, and different superscripts (a, b, c) indicate significant differences ($p < 0.05$).

BMSCs or BMSCs with osteogenic induction media to evaluate the *in vitro*, or *in vivo* osteogenesis of BMSCs combined with variable scaffolds (Kasten et al., 2003; Liu et al., 2008; Mauney et al., 2004, 2005; Yuan et al., 2007). Especially, *in vitro* osteogenesis induced MSCs prior to *in vivo* transplantation have been advantageous for rapid bone formation due to preformed calcified matrix. However, it is well known that undifferentiated MSCs have potential for differentiation into target cells after *in vivo* transplantation. Moreover, when MSCs were allowed to contact directly with a DBM scaffold, *in vitro* osteogenic differentiation was observed in non-osteogenic media (Kang et al., 2010; Mauney et al., 2004). In addition, MSCs seeded in scaffold had a limitation for the maintenance of viable cells in the interior of scaffold, because the preformed matrix might interrupt the permeability of supplying media (Mauney et al., 2004). It could be interpreted that blood supply might be disturbed by the over-generated matrix when the *in vitro* osteogenic differentiated cells and scaffolds were transplanted *in vivo*. These reasons suggest the significance of the present investigation on the osteogenic potential of undifferentiated MSCs, seeded in DBM prior to *in vivo* transplantation. Our findings showed not only a successful *in vitro* osteogenesis of hMSCs with DBM and fibrin glue scaffold, but also an enhanced *in vivo* osteogenesis of undifferentiated hMSCs when transplanted into the subcutaneous spaces with these scaffolds.

Interestingly, although all three types of hMSCs in this study showed similar cell proliferation rate *in vivo*, which was verified by the detection of PKH26 expression ratio to DAPI positive cells, the *in vivo* osteogenic potentials differed in each hMSCs groups. Indeed, hDFMSCs-grafted group showed the highest OC intensity and calcium content along with identical radiologic intensity to hBMSCs-grafted group. This could be related to the DBM scaffold and/or cell donor's age or gender, as the donors of hDFMSCs were younger than others in this study. However, if DBMs were properly processed, no direct relationship between osteogenic induction of DBMs and donor's age or gender was observed (Pietrzak et al., 2006; Traianedes et al., 2004). Moreover, DBM from the donors of bone pathologic conditions showed similar osteogenic potential compared to DBM from healthy donors (Liu et al., 2008). The other possible reason for these diverse osteogenic potentials between different hMSCs could be due to their variable characteristics (Morsczeck et al., 2009). These observations are supported by a recent study showing that proliferation and molecular signature of open chromatin of hBMSCs as determinants of heterotopic bone formation, and demonstrated a causal relationship between growth and engraftment of cell population (Janicki et al., 2011). In contrast to bone marrow, dental follicle is an ectomesenchymal tissue surrounding the developing tooth, and possesses the progenitors for osteoblasts of the alveolar bone as well as periodontal fibroblasts and cementoblasts (Morsczeck et al., 2008, 2009). In addition, dental follicle cells showed unique gene expression patterns before and after the osteogenic differentiation with stable expression of osteoblast specific transcription factors and differential expression or up-regulation of transcription factors, which promote the osteoblastic differentiation (Morsczeck et al., 2009). These results collectively suggested that hDFMSCs might have enhanced potential for osteogenic differentiation, even though the exact mechanism has not been clearly understood until now.

In conclusion, hMSCs derived from three different kinds of human somatic tissues, such as skin, bone marrow and dental follicle were able to differentiate *in vitro* into osteogenic cells when co-cultured with a DBM and fibrin glue scaffold. Moreover, successful *in vivo* osteogenesis of these hMSCs seeded in DBM prior to transplantation was observed in the subcutaneous tissues of athymic mice. Our findings suggest that hDFMSCs and hSMSCs with DBM scaffold can serve as an available substitute material, along with hBMSCs. Importantly, *in vivo* hDFMSCs-grafted group showed the highest OC expression and calcium content among the different hMSCs implanted specimens. Although further studies are needed, these results demonstrated that the dental follicle tissues could be used as an alternative autologous cell source for bone tissue engineering applications.

Acknowledgments

This work was supported by the Korea Research Foundation Grant funded by the Korean Government (KRF-2008-313-E00577 and NRF 2009-0071566) and the Gyeongsang National University Hospital Research Foundation Grant (GNUHCRF-2009-005).

References

Arrington, E.D., Smith, W.J., Chambers, H.G., Bucknell, A.L., Davino, N.A., 1996. Complications of iliac crest bone graft harvesting. Clinical Orthopaedics and Related Research 329, 300–309.

Blum, B., Moseley, J., Miller, L., Richelsoph, K., Haggard, W., 2004. Measurement of bone morphogenetic proteins and other growth factors in demineralized bone matrix. Orthopedics 27, s161–165.

Fernandes, K.J., Toma, J.G., Miller, F.D., 2008. Multipotent skin-derived precursors: adult neural crest-related precursors with therapeutic potential. Philosophical Transactions of the Royal Society of London—Series B: Biological Sciences 363, 185–198.

Gimble, J.M., Guilak, F., Nuttal, M.E., Sathishkumar, S., Vidal, M., Bunnel, B.A., 2008. In vitro differentiation potential of mesenchymal stem cells. Transfusion Medicine and Hemotherapy 35, 228–238.

Gronthos, S., Mankani, M., Brahim, J., Robey, P.G., Shi, S., 2000. Postnatal human dental pulp stem cells (DPSCs) in vitro and in vivo. Proceedings of the National Academy of Sciences of the United States of America 97, 13625–13630.

Gronthos, S., Brahim, J., Li, W., Fisher, L.W., Cherman, N., Boyde, A., DenBesten, P., Robey, P.G., Shi, S., 2002. Stem cell properties of human dental pulp stem cells. Journal of Dental Research 81, 531–535.

Janicki, P., Boeuf, S., Steck, E., Egermann, M., Kasten, P., Richter, W., 2011. Prediction of in vivo bone forming potency of bone marrow-derived human mesenchymal stem cells. European Cells & Materials 21, 488–507.

Jeon, O., Rhie, J.W., Kwon, I.K., Kim, J.H., Kim, B.S., Lee, S.H., 2008. In vivo bone formation following transplantation of human adipose-derived stromal cells that are not differentiated osteogenically. Tissue Engineering Part A 14, 1285–1294.
Jeon, B.G., Kang, E.J., Kumar, B.M., Maeng, G.H., Ock, S.A., Kwack, D.O., Park, B.W., Rho, G.J., 2011. Comparative analysis of telomere length, telomerase and reverse transcriptase activity in human dental stem cells. Cell Transplantation. doi:10.3727/096368911X565001.
Kaiser, S., Hackanson, B., Follo, M., Mehlhorn, A., Geiger, K., Ihorst, G., Kapp, U., 2007. BM cells giving rise to MSC in culture have a heterogeneous CD34 and CD45 phenotype. Cytotherapy 9, 439–450.
Kajahn, J., Gorjup, E., Tiede, S., von Briesen, H., Paus, R., Kruse, C., Danner, S., 2008. Skin-derived human adult stem cells surprisingly share many features with human pancreatic stem cells. European Journal of Cell Biology 87, 39–46.
Kanematsu, D., Shofuda, T., Yamamoto, A., Ban, C., Ueda, T., Yamasaki, M., Kanemura, Y., 2011. Isolation and cellular properties of mesenchymal cells derived from the deciduas of human term placenta. Differentiation 82, 77–88.
Kang, E.J., Byun, J.H., Choi, Y.J., Maeng, G.H., Lee, S.L., Kang, D.H., Lee, J.S., Rho, G.J., Park, B.W., 2010. In vitro and in vivo osteogenesis of porcine skin-derived mesenchymal stem cell-like cells with a demineralized bone and fibrin glue scaffold. Tissue Engineering Part A 16, 815–827.
Kasten, P., Luginbühl, R., van Griensven, M., Barkhausen, T., Krettek, C., Bohner, M., Bosch, U., 2003. Comparison of human bone marrow stromal cells seeded on calcium-deficient hydroxyapatite, beta-tricalcium phosphate and demineralized bone matrix. Biomaterials 24, 2593–2603.
Lindroos, B., Mäenpää, K., Ylikomi, T., Oja, H., Suuronen, R., Miettinen, S., 2008. Characterisation of human dental stem cells and buccal mucosa fibroblasts. Biochemical and Biophysical Research Communications 368, 329–335.
Liu, G., Sun, J., Li, Y., Zhou, H., Cui, L., Liu, W., Cao, Y., 2008. Evaluation of partially demineralized osteoporotic cancellous bone matrix combined with human bone marrow stromal cells for tissue engineering: an in vitro and in vivo study. Calcified Tissue International 83, 176–185.
Liu, G., Li, Y., Sun, J., Zhou, H., Zhang, W., Cui, L., Cao, Y., 2010. In vitro and in vivo evaluation of osteogenesis of human umbilical cord blood-derived mesenchymal stem cells on partially demineralized bone matrix. Tissue Engineering Part A 16, 971–982.
Mauney, J.R., Blumberg, J., Pirun, M., Volloch, V., Vunjak-Novakovic, G., Kaplan, D.L., 2004. Osteogenic differentiation of human bone marrow stromal cells on partially demineralized bone scaffolds in vitro. Tissue Engineering 10, 81–92.
Mauney, J.R., Jaquiéry, C., Volloch, V., Heberer, M., Martin, I., Kaplan, D.L., 2005. In vitro and in vivo evaluation of differentially demineralized cancellous bone scaffolds combined with human bone marrow stromal cells for tissue engineering. Biomaterials 26, 3173–3185.
Morsczeck, C., Götz, W., Schierholz, J., Zeilhofer, F., Kühn, U., Möhl, C., Sippel, C., Hoffmann, K.H., 2005. Isolation of precursor cells (PCs) from human dental follicle of wisdom teeth. Matrix Biology 24, 155–165.
Morsczeck, C., Schmalz, G., Reichert, T.E., Völlner, F., Galler, K., Driemel, O., 2008. Somatic stem cells for regenerative dentistry. Clinical Oral Investigations 12, 113–118.
Morsczeck, C., Schmalz, G., Reichert, T.E., Völlner, F., Saugspier, M., Viale-Bouroncle, S., Driemel, O., 2009. Gene expression profiles of dental follicle cells before and after osteogenic differentiation in vitro. Clinical Oral Investigations 13, 383–391.
Ock, S.A., Jeon, B.G., Rho, G.J., 2010. Comparative characterization of porcine mesenchymal stem cells derived from bone marrow extract and skin tissues. Tissue Engineering Part C Methods 16, 1481–1491.
Park, B.W., Hah, Y.S., Kim, D.R., Kim, J.R., Byun, J.H., 2007. Osteogenic phenotypes and mineralization of cultured human periosteal-derived cells. Archives of Oral Biology 52, 983–989.
Park, B.W., Kang, D.H., Kang, E.J., Byun, J.H., Lee, J.S., Maeng, G.H., Rho, G.J., 2012. Peripheral nerve regeneration using autologous porcine skin-derived mesenchymal stem cells. Journal of Tissue Engineering and Regenerative Medicine 6, 113–124.
Perka, C., Schultz, O., Spitzer, R.S., Lindenhayn, K., Burmester, G.R., Sittinger, M., 2000. Segmental bone repair by tissue-engineered periosteal cell transplants with bioresorbable fleece and fibrin scaffolds in rabbits. Biomaterials 21, 1145–1153.
Petite, H., Viateau, V., Bensaïd, W., Meunier, A., de Pollak, C., Bourguignon, M., Oudina, K., Sedel, L., Guillemin, G., 2000. Tissue-engineered bone regeneration. Nature Biotechnology 18, 959–963.
Phinney, D.G., Prockop, D.J., 2007. Concise review: mesenchymal stem/multipotent stromal cells: the state of transdifferentiation and modes of tissue repair—current views. Stem Cells 25, 2896–2902.
Pietrzak, W.S., Woodell-May, J., McDonald, N., 2006. Assay of bone morphogenetic protein-2, -4, and -7 in human demineralized bone matrix. Journal of Craniofacial Surgery 17, 84–90.
Reynolds, A.J., Jahoda, C.A., 2004. Cultured human and rat tooth papilla cells induce hair follicle regeneration and fiber growth. Differentiation 72, 566–575.
Riekstina, U., Muceniece, R., Cakstina, I., Muiznieks, I., Ancans, J., 2008. Characterization of human skin-derived mesenchymal stem cell proliferation rate in different growth conditions. Cytotechnology 58, 153–162.
Riekstina, U., Cakstina, I., Parfejevs, V., Hoogduijn, M., Jankovskis, G., Muiznieks, I., Muceniece, R., Ancans, J., 2009. Embryonic stem cell marker expression pattern in human mesenchymal stem cells derived from bone marrow, adipose tissue, heart and dermis. Stem Cell Reviews 5, 378–386.
Rogers, I., Yamanaka, N., Bielecki, R., Wong, C.J., Chua, S., Yuen, S., Casper, R.F., 2007. Identification and analysis of in vitro cultured CD-positive cells capable of multi-lineage differentiation. Experimental Cell Research 313, 1839–1852.
Schwarz, N., Redl, H., Schlag, G., Schiesser, A., Lintner, F., Dinges, H.P., Thurnher, M., 1989. The influence of fibrin sealant on demineralized bone matrix-dependent osteoinduction. A quantitative and qualitative study in rats. Clinical Orthopaedics and Related Research 238, 282–287.
Seo, B.M., Miura, M., Gronthos, S., Bartold, P.M., Batouli, S., Brahim, J., Young, M., Robey, P.G., Wang, C.Y., Shi, S., 2004. Investigation of multipotent postnatal stem cells from human periodontal ligament. Lancet 364, 149–155.
Toma, J.G., Akhavan, M., Fernandes, K.J., Barnabé-Heider, F., Sadikot, A., Kaplan, D.R., Miller, F.D., 2001. Isolation of multipotent adult stem cells from the dermis of mammalian skin. Nature Cell Biology 3, 778–784.
Traianedes, K., Russell, J.L., Edwards, J.T., Stubbs, H.A., Shanahan, I.R., Knaack, D., 2004. Donor age and gender effects on osteoinductivity of demineralized bone matrix. Journal of Biomedical Materials Research Part B: Applied Biomaterials 70, 21–29.
Wildemann, B., Kadow-Romacker, A., Haas, N.P., Schmidmaier, G., 2007. Quantification of various growth factors in different demineralized bone matrix preparations. Journal of Biomedical Materials Research Part A 81, 432–437.
Yamada, Y., Boo, J.S., Ozawa, R., Nagasaka, T., Okazaki, Y., Hata, K., Ueda, M., 2003. Bone regeneration following injection of mesenchymal stem cells and fibrin glue with a biodegradable scaffold. Journal of Cranio-Maxillofacial Surgery 31, 27–33.
Yuan, J., Cui, L., Zhang, W.J., Liu, W., Cao, Y., 2007. Repair of canine mandibular bone defects with bone marrow stromal cells and porous beta-tricalcium phosphate. Biomaterials 28, 1005–1013.